5

Retinal Identification

Mikael Agopov
University of Heidelberg
Germany

1. Introduction

Since the pioneering studies of Drs. Carleton Simon and Isodore Goldstein in 1935 [Simon & Goldstein (1935)], it has been known that every eye has its own unique pattern of blood vessels, and that retinal photographs can be used for identifying people. In the 1950's, this was proven to hold even for identical twins [Tower (1955)]. Hence the idea of using the retinal blood vessel pattern for identification. Eye fundus photography for the purpose of identification is impractical, however. An optical device which scans the retinal blood vessel pattern is required.
Such an optical Retinal Identification (RI) device was originally patented in 1978 [Hill (1978)]; after several subsequent patents, it developed into a commercial product in the 1980s and 1990s. As the patent of retinal identification (opposed to the actual design of the device) has now worn off, new developments in the field have taken place. In this chapter, the history, technique and recent developments of RI are discussed.

1.1 The anatomy and optical properties of the human eye

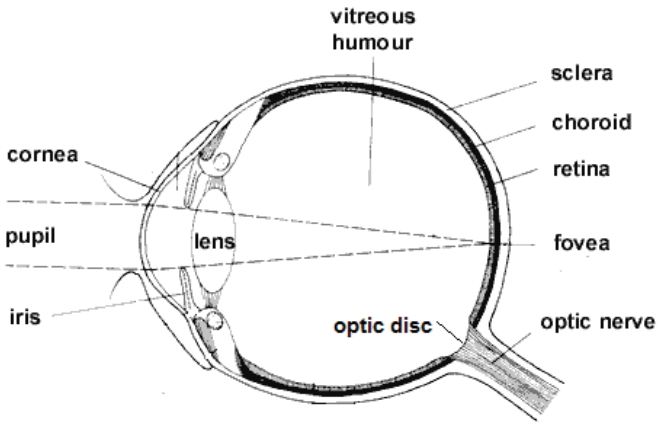

Fig. 1. A schematic picture of the human eye.

A schematic picture of the human eye is shown in Figure 1. The eyeball is of about 24 mm in diameter and filled with *vitreous humor*, jelly-like substance similar to water; its outer shell, the *sclera*, is made of rigid proteins called collagen. The light entering the eye first passes through the *pupil*, an aperture-like opening in the *iris*. The size of the pupil limits the amount of light entering the eye. The light is focused by the *cornea* and the *crystalline lens* onto the *retina*. The retina converts the photon energy into an electric signal, which is transferred to the brain through the *optic nerve*.
The cornea is about 11 mm in diameter and only 0.5 mm thick. It accounts for most of the refractive power of the eye (about 45 D). The remaining 18 D come from the crystalline lens, which is also - through deformation - able to change its refractive power, thus partly compensating for the refractive error and helping to focus the eye.
The retina is a curved surface in the back of the eye. The point of sharpest vision is called *fovea* - here the light-sensing *photoreceptor cells* are only behind a small number of other cells. Elsewhere on the retina, the light has to travel through a multi-layered structure of different cells. These various cells are responsible for the eye's 'signal processing', i.e. turning the incoming photons first into a chemical and then to an electric signal.
After being amplified and pre-processed, the signal is transferred to the nerve fibers, which reside on the peripheral area of the retina around the *optic disc*, where they form the *retinal nerve fiber layer* (RNFL). The optic disc is an approximately $5^\circ \times 7^\circ$, ellipse-like opening in the eye fundus, through which the nerve fibers and blood vessels enter the eyeball. It is about 15° away from the fovea in the nasal direction. The *choroid* is the utmost layer behind the retina just in front of the sclera. It has a bunch of small blood vessels, and is responsible for the retina's metaboly.

1.2 The birefringence properties of the eye

Birefringence is a form of optical anisotrophy in a material, in which the material has different indices of refraction for p- and s-polarization components of the incoming light beam. The components are thus refracted differently, which in general results the beam being divided into two parts. If the parts are then reflected back by a diffuse reflector (such as the eye fundus), a small portion of the light will travel the same way as it came, joining the polarization components into one again, but having changed the beam's polarization state in process[1].
The birefringence of the eye is well documented (Cope et al. (1978), Klein Brink et al. (1988), Weinreb et al. (1990), Dreher et al. (1992)). The birefringence of the corneal collagen fibrils constitutes the main part of the total birefringence of the eye. Its amount and orientation changes throughout the cornea. In the retina, the main birefringent component is the retinal nerve fiber layer (RNFL), which consists of the axons of the nerve fibers. The thickness of RNFL is not constant over the retina; the amount of birefringence varies according to the RNFL thickness and also drops steeply if a blood vessel (which is non-birefringent) is encountered.
The most successful application of measuring the RNFL thickness around the optic disc is probably the GDx glaucoma diagnostic device (Carl Zeiss Meditec, Jena, Germany). It uses scanning laser polarimetry to topograph the RNFL thickness on the retina. A reduced RNFL thickness means death of the nerve fibers and thus advancing glaucoma. A typical GDx image is shown in Figure 2.

[1] See Appendix about how the polarization change can be measured.

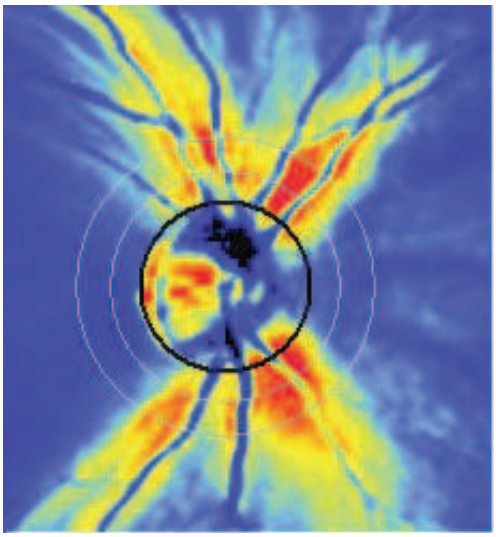

Fig. 2. A typical GDx image of a healthy eye. The birefringent nerve fiber layer is seen brightly in the image, as well as the blood vessels which displace the nerve fibers, thus resulting in a weaker measured signal (darker in the image).

2. RI using retinal blood vessel absorption

The first patent of the biometric identification using the retinal blood vessel pattern dates back to 1978 [Hill (1978)]. Soon afterwards, the author of the patent founded the company EyeDentity (then Oregon, Portland, USA) and began full-time efforts to develop and commercialize the technique.

In the original patent, the retinal blood vessel pattern is scanned with the help of two rings of LEDs. The amount of light reflected back from the retina is measured - when the beam hits a blood vessel, it is absorbed to a bigger extent than when it hits other tissue. In the original retina scan, green laser light was used - it was strongly absorbed by the red blood vessels. However, it was found out that visible light causes discomfort to the identified individual, as well as pupil constriction, causing loss of signal intensity.

Since the first working prototype RI, patented in 1981 [Hill (1981)], near-infrared (NIR) light has been used for illumination. The infrared light is not absorbed by the photoreceptors (the absorption drops steeply above 730 nm); however, the retinal blood vessels are fairly transparent to the NIR wavelengths as well - the light is absorbed by the smaller choroidal blood vessels instead (thus, considering this technique, the term *Retinal Identification* is slightly misleading) before being reflected back from the eye fundus. The image acquisition technique has also been changed: the LEDs are given up in favour of scanning optics. A circular scan is preferred over a raster, which suffers from the problem of reflections from the cornea.

In the patent of 1986 [Hill (1986)], the scan is centered around the fovea instead of the optic disc. The fovea is on the optical axis of the eye, so this arrangement has the definite advantage that no fixation outside the normal line of sight is required, unlike when a ring around the optic disc is scanned, when the subject has to look 15 degrees off-axis. The downside is that

the choroidal blood vessels are much thinner than around the optic disc, and they don't form a clear pattern. Thus the price paid for easier fixation is the quality of the signal.

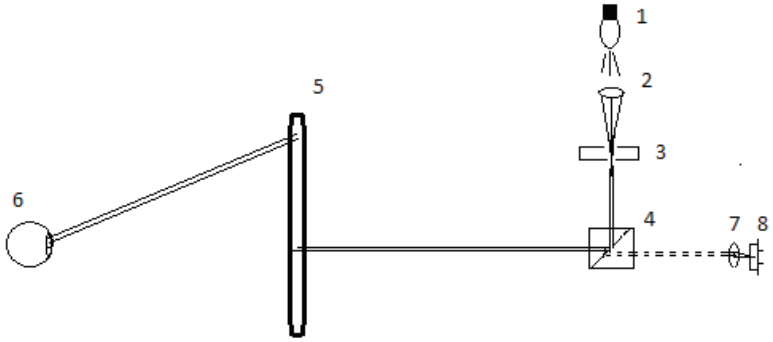

Fig. 3. A schematic drawing of the current Retinal Identification technique, based on the patent from 1996. A detailed explanation is in the text.

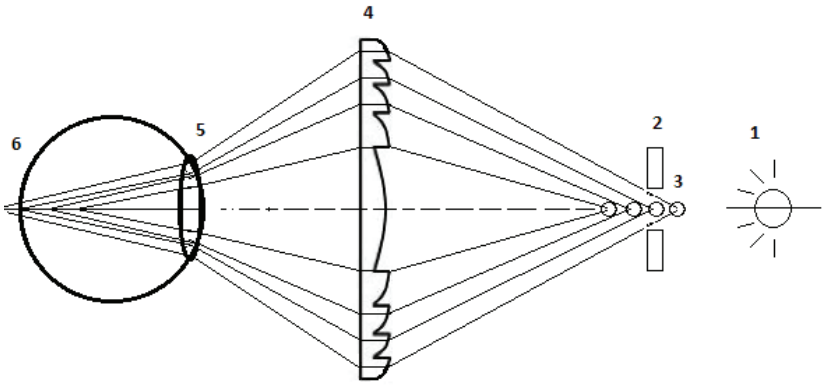

Fig. 4. A schematic drawing fixation-alignment technique using a Fresnel lens. A detailed explanation is in the text.

Current RI technology is based on an active US patent [Johnson & Hill (1996)]. A schematic drawing of the measurement setup is shown in Figure 3. An infrared light source, for example a krypton lamp (1), is focused by a lens (2) through an optical mirror (explained below) via a pinhole (3). The light enters a beam splitter (4) which reflects it into a Fresnel optical scanner (5). The rotating optical scanner scans a ring on the cornea, which - if properly focused - will hit the retina at the same angle. A multifocus Fresnel lens, cemented in the scanner, creates a fan of nearly-collimated light beams which hit the eye of the tested subject. One of the

beams will be focused on the retina by the eye's own optical apparatus, thus compensating for refractive error (explained in detail below).
The light reflected back from the eye fundus travels the same way through the scanner and into the beam splitter; a part of it is transmitted into a photodetector (8) through a focusing lens (7). After being measured by the photodetector, the signal is A/D-converted, amplified and processed. The processed signal is converted into points, which are stored in an array, which is used for matching. A similar process is used in all RI techniques.
Fixation and alignment of the subject's eye in a RI measurement is critical; it is almost impossible to scan a non-willing subject. The fixation system of the RI technique, which was also patented (Arndt (1990)) , is illustrated in Figure 4. A Light-Emitting Diode (LED) is situated next to the Krypton lamp. It illuminates the optical double-surface mirror, creating several reflections, 'ghost images', of the LED on the optical axis of the system. These images function as targets for the test subject's eye. The eye looks at them through a multifocal Fresnel lens. The lens, which consists of several focusing parts with different focal lengths, focuses the ghost images on different points on the eye's optical axis. Regardless of whether the test subject is emmetropic (normal visual acuity), myopic (near-sighted) or hyperopic (far-sighted), one of the images will almost certainly end up on the retina and will thus result a sharp image and effectively compensate for the refractive error of the subject's eye. However, this happens at the cost of optical image quality; the measured pattern is a sum of contributions from choroidal blood vessels and other structures.

2.1 Matching

At first, a reference measurement, which the further measurements will be compared against, has to be taken from each tested subject. Any further measurement will be compared against the reference. As the subject's eye can rotate around the optical axis (due to different head position, i.e. head tilt, between the measurements), the best possible match is found by 'rotating' the measurement points in the array. The matching is done using a Fourier-based correlation; the match is measured on a scale of +1,0 (a perfect match) to -1,0 (a complete mismatch). User experience has shown that a match above 0,7 can be considered a matching identification.

3. RI using the RNFL birefringence

The blood vessels emerging into the retina through the optic disc often displace the nerve fibers in the retinal nerve fiber layer. Unlike the RNFL nerve fiber axons, the blood vessels are not birefringent - thus, if the birefringence (change in the state of polarization) of the scanning laser beam is measured around the optic disc, a steep signal drop proportional to the blood vessel size is measured wherever one is encountered. This can be seen in the GDx-pictures, where the blood vessels are seen as dark lines on the otherwise bright nerve fiber layer.
The author and his co-workers studied the possibility of using blood vessel-induced RNFL birefringence changes for biometric purposes [Agopov et al. (2008)]. A measurement device was built to scan a circle of 20° around the optic disc. The measured birefringence would drop steeply where a blood vessel is encountered, creating a sharp drop, or 'blip', in the measured signal. The scanning angle is big enough to catch the major blood vessels which enter the fundus through the disc.

3.1 Apparatus and method

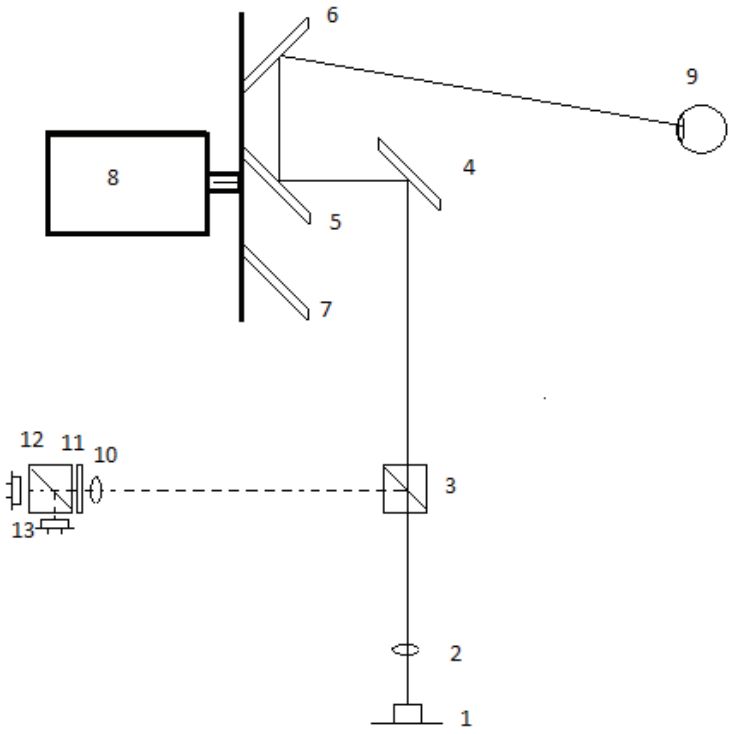

Fig. 5. A schematic drawing of the RI measurement setup using the RNFL birefringence. A detailed explanation is in the text.

The measurement setup is explained in detail in [Agopov et al. (2008)]; here it is explained briefly. The apparatus and the light paths within it are shown in Figure 5. The light path is drawn with a solid line. A 785 nm laser diode (1) was used as a light source. The beam was collimated by a lens (2); then it passed through a non-polarizing beam splitter (3) and was reflected by a mirror (4) further into the optical scanner (5-8). The two scanning mirrors (5 and 6) and a counterweight (7) were cemented on an aluminium plate which was spun by a DC motor (8). The center mirror was (5) tilted 45° from the disc plane rotated clockwise and reflected the laser beam onto the edge mirror. The edge mirror (6) was tilted 50°, creating a circular scan subtending a 10° radius of visual angle (20° diameter) in the tested subject's eye (9). The reflection from the ocular fundus traveled back the same optical path through the scanner; now, however, the beam splitter (3) reflected the useful half of the beam (drawn with dashed line) into the detection system (10-13). A lens (10) focused the beam into a polarizing beam splitter (12) through a quarter wave plate (11) which had its fast axis 45° to the original plane of polarization. The polarizing beam splitter separated the p- and s-polarization components; two avalanche photodiodes (13) were placed right after it, measuring the two signals which corresponded the two polarization components. Amplified by the detection electronics, the signals were added and subtracted

respectively. The polarization was manipulated so that the Stokes parameters S_0 and S_3 were measured - it was decided to measure S_3 instead of S_1 for birefringence-based changes as it appeared to suffer less from various amounts and orientations of corneal birefringence in our computerized model.
As the alignment of the eye is critical, special care was taken to properly align the test subject's eye. The measurement apparatus included three eyepieces: the measurement was taken through the fixed central piece; in addition there were two horizontally movable ones; the subject could look through the central piece with either eye while having a 'dummy' eyepiece available for the other eye. Thus possible head tilt was reduced to almost zero.
Because the fixation point of the retina, the fovea, is approximately 15 degrees away from the optic disc, the measured eye had to look 15° away in the nasal direction to center the scan on the optic disc. To achieve this, two fixation LEDs were set at 15° angle to the central axis of the scan. Because the human eye is about 0,75 D myopic at the wavelength 785 nm (see [Fernandez et al. (2005)] for details) the fixation LEDs were placed at 130 cm distance, so that the eye's fixation would compensate for this.

4. RI using the optic disc structure

Another interesting RI technology was patented in 2004 [Marshall & Usher (2004)]. The idea is to use the image of the optic disc - taken by a scanning laser ophthalmoscope (SLO) - for identification. A company Retinal Technologies (Boston, MA, USA) was founded for developing the technique.

4.1 The principle of an SLO

The best-known application of the SLO is probably the Heidelberg Retina Tomograph (Heidelberg Engineering, Heidelberg, Germany), which is used for glaucoma diagnostics. The principle of an SLO is illustrated in 6. A low-intensity laser diode (1) is used for illumination. A collimated laser beam goes through a beam splitter (2) into an optical scanner (3). The scanner consists of two rotating mirrors, a fast and a slow one, creating a raster scan. The scanning beam is imaged through two lenses (4 and 5) onto exactly one point called the *conjugated plane*. If the imaged subject's cornea is at this point(6), the eye's optics focus the scanning beam onto the retina (7). The reflection from the eye fundus travels back through the system, but is reflected into the detection system (7-9) by the beam splitter. A lens (7) focuses the beam through a pinhole (8) onto a photodiode (9). The pinhole is very important - only the light which comes exactly from the conjugated plane reaches the photodetector. Thus the SLO creates a high-resolution microscopic image of the retina. The scan is usually centered around the optic disc (using an off-axis fixation target - as in the previous setup). A typical SLO image of the optic disc (taken with the HRT) is shown in Figure 7.

4.2 Image analysis

The boundary of the optic disc is found from the image taken by the SLO. There is a clear boundary between the disc and surrounding tissue (as seen in Figure 7); an ellipse is fit onto the image by analyzing the average intensity of the pixels around the boundary.
Once the disc is identified, a recognization pattern is created from the its structures. This fairly complicated procedure is explained in detail in the patent. The patterns of recognized

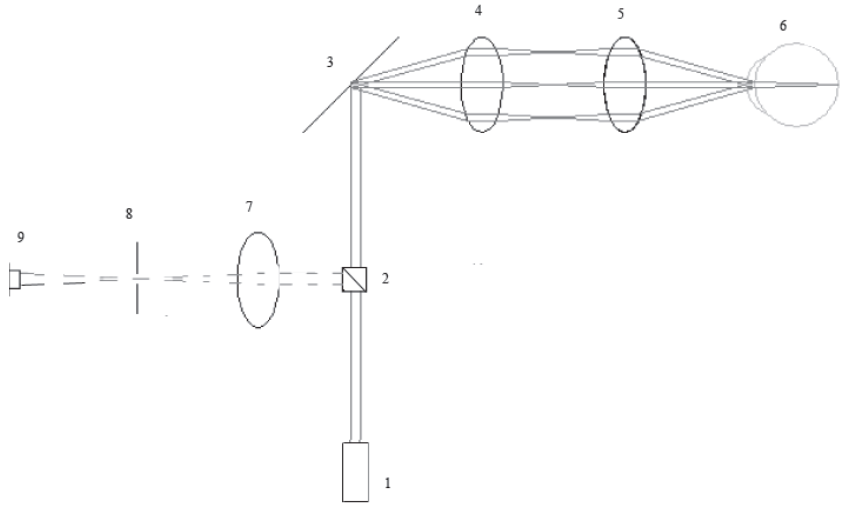

Fig. 6. An schematic drawing of a scanning laser ophthalmoscope. A detailed explanation is in the text.

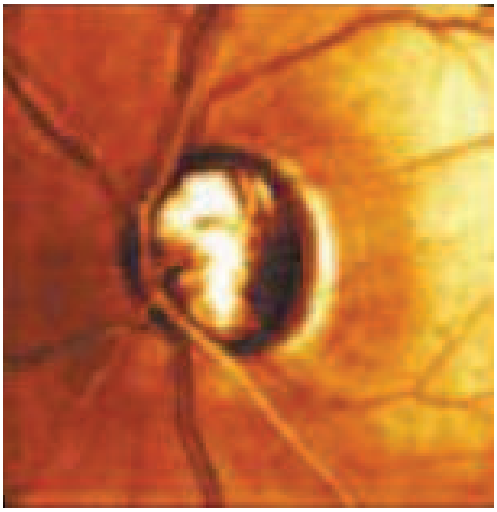

Fig. 7. A typical SLO image of the optic disc (taken with an HRT).

individuals are stored in a database for comparing with the pattern of a person wishing to be identified.

5. Combined retina and iris identification

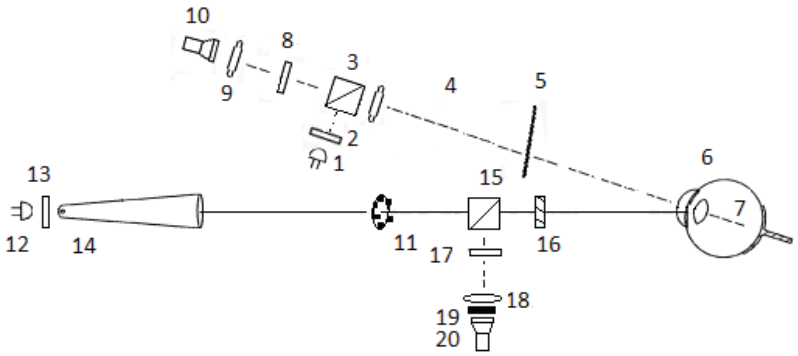

Fig. 8. The measurement setup of a combined retina and iris identification device. The details are in the text.

In a fairly recent patent [Muller et al. (2007)], a combination of retina and iris identification was suggested (about iris identification, see the previous chapter). The measurement system is constructed so that both biometrics can be recorded with one scan. This is obviously advantageous, as now two biometrics are available simultaneously. The measurement setup is shown in Figure 8. The setup has two optical axes: one for the retinal image (dashed line) and one for alignment and the iris image (solid line). They are 15° apart; as explained earlier, the incoming light is focused on the area around the optic disc only if the eye is looking 15° in the nasal direction. To achieve this, the test subject has to be faced towards the dashed line but look in the direction of the solid line. As a fixation target, a ring of green LED's (11) is placed around the optical axis of the iris scanning system.
Two illuminating LED's are used: One infrared ($\lambda \approx 800$ nm) LED (1), and one red ($\lambda \approx 660$ nm) LED (12). The interference from the 'wrong' light source is blocked a dichroic mirror (5). The light from the infrared LED (1) first goes through a polarizer (2), which ensures that the outgoing light is linearly polarized. The outgoing beam is then divided into two parts by a beam splitter (3). The transmitted (useless) part crosses the beam splitter and is preferably absorbed by a light trap. The reflected (useful) beam part is collimated by a lens (4) and goes through the dichroic mirror (5) into the eye. The beam is focused by the eye's optics (6) onto the area around the optic disc; after being reflected from the eye fundus (7), a reflection of the beam returns back the same way as the beam came; however, coming from the other direction, a part of the reflected beam now passes through the beam splitter into the detection system. The polarizer (8) is set so that it absorbs the illuminating LED's polarization direction. However - having changed its state of polarization while passing through the eye tissue - a part of the beam is now able to pass through the polarizer. The beam is focused by a lens (9) onto the detector (10), which can be for example a CCD camera. It should be noted that this setup has no optical scanner (nor it is confocal) - a wide-field image around the optic disc is

captured, thus resulting in lower resolution than a confocal scanning system would achieve.
For the iris scan, the illuminating light from the red LED (12) is first linearly polarized (13) [2]. and then guided into the eye through an alignment tube (14). The function of the alignment tube is not explained in the patent; preferably it would consist of at least one lens with a long focal length, which would focus the light onto the iris (the beam entering the eye should not be parallel, otherwise it will be focused on the retina). The distance between the lens and the beam splitter should be much bigger than that between the beam splitter and the eye, so that the slightly de-focused reflection image of the iris can be caught. On its way to the iris and back, the light double-passes a quarter wave plate (16). The wave plate's axes are set so that both the fast and the slow axis of it are 45° to the original polarization direction - when the beam passes through it, its polarization becomes circular; the second pass (the reflection from the iris) turns the circular polarization into linear again, but having turned the polarization direction by 90° in the process. After entering the detection system (17-20), the light can now pass through the polarizer (17), which is set to absorb the polarizing direction of the initial polarizer (13). The beam is focused by a lens onto the detector (a CCD camera); the possible reflections of the green LED are filtered out by a red band pass filter (19).
The two detection systems are electronically synchronized so that one scan records both images simultaneously. The recording is triggered by a switch, which is turned on when the eye is correctly aligned.
The eye is at a crossing of two optical axes - its distance and orientation are critical. In the setup suggested in the patent, the distance is controlled by an ultrasound transducer. It sends and receives ultrasound pulses which are reflected back from the surface of the cornea. When the distance is right, and the optic disc is seen on the CCD (10), the eye is aligned properly, and the recording can be taken.

6. Results of performance tests and limitations of the RI techniques

6.1 RI using absorption

In a performance test by Sandia National Laboratories [Sandia Laboratories (1991)], the EyeDentity RI device recognized >99% of the tested subjects in a three-attempt measurement, with no false positives.

6.1.1 Limitations

As the light has to pass twice through the pupil during the measurement, a constricted pupil can increase the number of false negative scan results. Thus dim light conditions are preferable for the RI (of course, this is true for almost any optical measurement); the technique has difficulties in broad daylight. In addition, various eye conditions can disturb the light's passing through the eye, compromising vision; this also affects measuring the eye's properties optically, including the RI.

[2] In the patent, the device is desribed without the polarizers (13 and 17), the quarter wave plate (16), the filter (19); instead of a beam splitter (15), a dichroic mirror is suggested. The fixation LEDs are also placed together with the red illuminating LED. However, this leads to unsurmountable difficulties. First of all, the IR light and the green light used for fixation cannot *both* pass through the dichroic mirror; moreover, the IR light would first have to *pass* through the mirror - the reflection from the eye would then have to be *reflected* by it. Therefore, the author suggests slight modifications in the setup.

1. Severe astigmatism: An astigmatic eye's optics image dots as lines. This results in problems with focusing and also bad optical quality of measurements.
2. Cataracts: A cataract is an eye condition in which clouding develops in the crystallinen lens. The lens becomes opaque so seeing becomes compromised. Obviously any optical measurement in the eye, including the RI, becomes increasingly difficult.
3. Severe eye diseases, such as the age-related macula degeneration (AMD), can change the structure of the retina, either by destroying retinal tissue or by stimulating growth of new blood vessels.

6.2 RI using birefringence

Eight eyes of four volunteer subjects were measured. Both absorption- and birefringence-based signals were recorded two times for each eye. For verifying purposes, fundus photographs were taken from all the eyes. The measured peaks and the blood vessels on the fundus photos were compared as follows:
A 20° diameter circle was drawn on a transparent overlay, on which the measured peaks were marked at corresponding angles on the perimeter of the circle. The transparency was then placed on the fundus photo to compare the marked signal peaks with the blood vessels on the photo. Only the vessels larger than a certain threshold size (set for each eye individually) were taken into account, i.e. the smallest vessels were ignored. In this way, the numbers of blood vessels corresponding to the peaks in the measured absorption/reflectance and birefringence-based tracings were calculated. If a confirmed peak did not correspond to a vessel above the threshold size on the fundus photo, it was considered a false positive.
Altogether 55 blood vessels were located on the fundus photos of the 'better' eyes (the ones which yielded clearer signals) of the four volunteers, of which 34 could be correlated with the 'peaks' in the measured signal. The calculated sensitivities (number of vessels identified / number of vessels altogether) and specificities (number of positive recognitions / number of positive + false positive recognitions) - are presented in Table 1. The columns in the tables represent total percentage of blood vessel 'peaks' correlating with vessels in the fundus photo (Total), from the two reflection/absorption measurements (Sum) and from the two birefringence measurements (Diff).

	Total	Sum	Diff
Average sensitivity	69%	51%	33%
Average specificity	78%	76%	60%

Table 1. Summarized results of the measurements taken from the eye with a better signal of each subject.

6.2.1 Limitations

Our system was of 'proof-of-principle' -nature and - unlike the conventional RI technique - had no inherent defocus compensation; the test subjects were required to have a refractive error of less than about ± 2 diopters or a good corrected vision using contact lenses. The eye conditions disturbing the measurement include cataracts and astigmatism as well as a severe glaucoma, which damages the RNFL by killing the nerve fibers going through the optic nerve.

6.3 Other techniques

The author in unaware of any scientific studies on the accuracy of the other techniques mentioned here.

7. Discussion

Retinal Identification remains the most reliable and secure biometric. Falsifying an image of a retinal blood vessel pattern appears impossible. The eye scans are generally considered invasive or even harmful, especially if a laser (even if the light is weak intensity and harmless to the eye, as in our system). However, the enrollees should be able to overcome their fear of these scans once they acquire more user experience.

The original RI technique uses the choroidal blood vessel pattern for identification; however, several newer RI techniques center the scan around the optic disc. The main drawback in such a device is that the eye has to fixate 15 degrees off-axis while being measured. However, if this is achieved, the blood vessels around the optic disc are easier to detect - in addition, the - as the authors and his co-workers proved - birefringence-based blood vessel detection can help detecting more blood vessels, only at a small cost of specificity. The measured signal was also directly linked to blood vessels and not to other retinal structures, as in the original RI technique.

The newer techniques - imaging the optic disc using an SLO, or the combined retina- and iris scan - appear very promising. However, the author is unaware either of any commercial devices or of any scientific studies on the accuracy of these identifying method.

The use of retinal identification is not limited to humans. In 2004, a patent was filed on identifying various animals using their retinal blood vessel pattern [Golden et al. (2004)]. To develop the technique for animals, a company OptiBrand was started (Ft. Collins, Colorado, USA). The company produces and develops hand-held video camera -based devices which provide an acceptable image an animal's eye fundus to allow identification. This method is certainly preferable over the traditional hot iron branding, which is not only painful to the animal, but also costly in the lost hide value. When a false identification is not disastrous (as opposed to some high security installations), a simple video camera based device provides an accurate enough identification.

8. Appendix: The Stokes parameters

The modern treatment of polarization was first suggested by Stokes in the mid-1800's. The polarization state of the light can be completely represented with four quantities, the *Stokes parameters*:

$$\begin{aligned} S_0 &= \langle E_x^2 \rangle_T + \langle E_y^2 \rangle_T \\ S_1 &= \langle E_x^2 \rangle_T - \langle E_y^2 \rangle_T \\ S_2 &= \langle 2E_x E_y \cos\epsilon \rangle_T \\ S_3 &= \langle 2E_x E_y \sin\epsilon \rangle_T, \end{aligned} \tag{1}$$

where $\epsilon = \epsilon_y - \epsilon_x$ is the phase difference between x- and y-polarization and the $\langle\rangle_T$ denote time averages.

For totally unpolarized light $S_0 > 0$ and $S_1 = S_2 = S_3 = 0$. For completely polarized light, on

the other hand, $S_0^2 = S_1^2 + S_2^2 + S_3^2$. The polarization state of the light can be defined as

$$V = \frac{\sqrt{S_1^2 + S_2^2 + S_3^2}}{S_0}. \tag{2}$$

The importance of the Stokes parameters lies in the fact that they are connected to easily measurable intensities:

$$\begin{aligned} S_0(\theta,\rho) &= I(0^\circ,0) + I(90^\circ,0) \\ S_1(\theta,\rho) &= I(0^\circ,0) - I(90^\circ,0) \\ S_2(\theta,\rho) &= I(45^\circ,0) - I(135^\circ,0) \\ S_3(\theta,\rho) &= I(45^\circ,\pi/2) - I(135^\circ,\pi/2), \end{aligned} \tag{3}$$

where θ is the angle of the azimuth vector measured from the x-plane and ρ is the birefringence. These can be easily measured: for example, S_1 can be measured with polarizing beam splitter and two detectors, which are placed so that they measure the intensities coming out of the beam splitter, and S_3 can be measured by adding a quarter wave plate before the aforementioned system.

9. References

Agopov, M.; Gramatikov, B.I.; Wu, Y.K.; Irsch, K; Guyton, D.L. (2008). Use of retinal nerve fiber layer birefringence as an addition to absorption in retinal scanning for biometric purposes. *Applied Optics* 47: 1048-1053

Bettelheim, F. (1975). On optical anisotrophy of the lens fiber cells. *Exp. Eye Res.* 21: 231-234

Cope, W.; Wolbarsht; Yamanashi, B. (1978). The corneal polarization cross. *J. Opt Soc Am* 68: 1149-1140

Dreher, A.; Reiter, K. (1992). Scanning laser polarimetry of the retinal nerve fiber layer. *SPIE* 1746:34-41

Fernandez, E. J.; Unterhuber, A; Pieto, P.M.; Hermann, B.; Drexler, W.; Artal, P. (2005). Ocular aberrations as a function of wavelength in the near infrared measured with a femtosecond laser. *Optics Express* 13:400-409

Hill, R. (1978). Apparatus and method for identifying individuals through their retinal vasculature patterns, *United States Patent* 4109237

Hill, R. (1981). Rotating beam ocular identification apparatus and method. *United States Patent* 4,393,366

Hill, R. (1986). Fovea-centered eye fundus scanner. *United States Patent* 4620318

Johnson, J.C.; Hill, R. (1996). Eye fundus optical scanner system and method, *United States Patent* 5532771

Golden, B.L.; Rollin, B.E.; Switzer, R.; Comstock, C.R. (2004). Retinal vasculature image acquisition apparatus and method, *United States Patent* 6766041

Arndt, J.H. (1990). Optical alignment system. *United States Patent* 4923297

Klein Brink, H. B.; Van Blockland, G.J. (1988). Birefringence of the human foveal area assessed in vivo with the Mueller-Matrix ellipsometry. *J. Opt. Soc. Amer.* A 5:49-57

Marshall, J.; Usher, D. (2004). Method for generating a unique and consistent signal pattern for identification of an individual, *United States Patent* 6757409

Muller, D. F.; Heacock G. L.; Usher D. B. (2007). Method and system for generating a combined retina/iris patter biometric, *United States Patent* 7248720

Sandia National Laboratories (1991). Performance Evaluation of Biometric Identification Devices, *Technical Report SAND91-0276, UC-906*

Simon C.; Goldstein I. (1935). A New Scientific Method of Identification, *New York State Journal of Medicine*, Vol. 35, No. 18, pp. 901-906

Tower, P. (1955). The fundus Oculi in monozygotic twins: Report of six pairs of identical twins, *Archives of Ophthalmology*, Vol. 54, pp. 225-239

Weinreb, R.; Dreher A.; Coleman, A.; Quigley H.; Shaw, B.; Reiter, K. (1990). Histopatologic validation of Fourier-ellipsometry measurements of retinal nerve fiber layer thickness, *Arch Opthalmol* 108:557-60

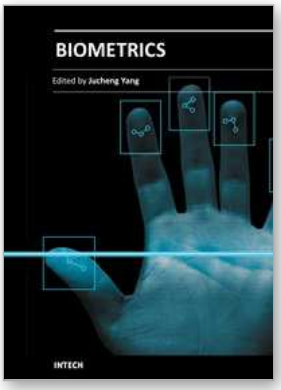

Biometrics

Edited by Dr. Jucheng Yang

ISBN 978-953-307-618-8
Hard cover, 266 pages
Publisher InTech
Published online 20, June, 2011
Published in print edition June, 2011

Biometrics uses methods for unique recognition of humans based upon one or more intrinsic physical or behavioral traits. In computer science, particularly, biometrics is used as a form of identity access management and access control. It is also used to identify individuals in groups that are under surveillance. The book consists of 13 chapters, each focusing on a certain aspect of the problem. The book chapters are divided into three sections: physical biometrics, behavioral biometrics and medical biometrics. The key objective of the book is to provide comprehensive reference and text on human authentication and people identity verification from both physiological, behavioural and other points of view. It aims to publish new insights into current innovations in computer systems and technology for biometrics development and its applications. The book was reviewed by the editor Dr. Jucheng Yang, and many of the guest editors, such as Dr. Girija Chetty, Dr. Norman Poh, Dr. Loris Nanni, Dr. Jianjiang Feng, Dr. Dongsun Park, Dr. Sook Yoon and so on, who also made a significant contribution to the book.

How to reference

In order to correctly reference this scholarly work, feel free to copy and paste the following:

Mikael Agopov (2011). Retinal identification, Biometrics, Dr. Jucheng Yang (Ed.), ISBN: 978-953-307-618-8, InTech, Available from: http://www.intechopen.com/books/biometrics/retinal-identification

INTECH
open science | open minds

InTech Europe
University Campus STeP Ri
Slavka Krautzeka 83/A
51000 Rijeka, Croatia
Phone: +385 (51) 770 447
Fax: +385 (51) 686 166
www.intechopen.com

InTech China
Unit 405, Office Block, Hotel Equatorial Shanghai
No.65, Yan An Road (West), Shanghai, 200040, China
中国上海市延安西路65号上海国际贵都大饭店办公楼405单元
Phone: +86-21-62489820
Fax: +86-21-62489821